

Supplementary Materials

The Design Strategy for an Aggregation- and Crystallization-Induced Emission-Active Molecule Based on the Introduction of Skeletal Distortion by Boron Complexation with a Tridentate Ligand

Shunsuke Ohtani, Masayuki Gon, Kazuo Tanaka* and Yoshiki Chujo

Department of Polymer Chemistry, Graduate School of Engineering, Kyoto University
Katsura, Nishikyo-ku, Kyoto 615-8510, Japan; ohtani@poly.synchem.kyoto-u.ac.jp (S.O.);
gon@poly.synchem.kyoto-u.ac.jp (M.G.); chujo@poly.synchem.kyoto-u.ac.jp (Y.C.)

* Correspondence: tanaka@poly.synchem.kyoto-u.ac.jp

Contents:	page
General	S–2
Materials	S–3
Synthesis of 1	S–4
Synthesis of 2	S–5
Synthesis of 3 and BPhQ	S–6
Synthesis of 5 , 6 and BPhQm	S–9
Single-crystal X-ray structure analysis of BPhQ and BPhQm	S–12
Optical Measurements Data	S–14
Computational Details	S–18
References	S–18

1. General

^1H (400 MHz), ^{13}C (100 MHz), and ^{11}B (128 MHz) NMR spectra were recorded on JEOL JNM-AL400 or JNM-EX400 spectrometers. The samples were analyzed in CDCl_3 . The chemical shift values were expressed relative to tetramethylsilane (TMS) for ^1H and ^{13}C NMR as an internal standard in CDCl_3 and $\text{BF}_3\cdot\text{OEt}_2$ for ^{11}B NMR as a capillary standard. Analytical thin-layer chromatography (TLC) was performed with silica gel 60 Merck F254 plates. Column chromatography was performed with Wakogel® C-300 silica gel. High-resolution mass (HRMS) spectrometry was performed at the Technical Support Office (Department of Synthetic Chemistry and Biological Chemistry, Graduate School of Engineering, Kyoto University), and the HRMS spectra were obtained on a Thermo Fisher Scientific EXACTIVE spectrometer for electrospray ionization (ESI). The UV–vis–NIR absorption spectra were recorded on a SHIMADZU UV-3600 spectrophotometer, and the samples were analyzed at room temperature. The photoluminescence (PL) spectra were measured on a HORIBA JOBIN YVON Fluoromax-4P spectrofluorometer. The absolute PL quantum efficiency was measured on a Hamamatsu Photonics Quantaaurus-QY Plus C13534-01. The PL lifetime measurement was performed on a Horiba FluoroCube spectrofluorometer system; excitation was carried out using a UV diode laser (NanoLED 375 nm). An X-ray crystallographic analysis was carried out by Rigaku R-Axis RAPID-F imaging plate diffractometer with graphite-monochromated $\text{MoK}\alpha$ radiation and Rigaku Saturn 724+ with a MicroMax-007HF CCD diffractometer with Varimax Mo optics using graphite-monochromated $\text{MoK}\alpha$ radiation. The analysis was carried out with direct methods (SHELX-2014/7) using Yadokari-XG. The program Mercury 3.3.1 was used to generate the X-ray structural diagram.

2. Materials

2.1. Commercially available compounds used without purification:

4-*tert*-Butylanisole (Tokyo Chemical Industry Co, Ltd.),
Bromine (Wako Pure Chemical Industries, Ltd.),
NaHSO₃ (Wako Pure Chemical Industries, Ltd.),
Na₂SO₄ (Wako Pure Chemical Industries, Ltd.),
1.64 M *n*-BuLi *n*-hexane solution (Kanto Chemical Co., Inc.),
8-Methoxyquinoline (Tokyo Chemical Industry Co, Ltd.),
Mg₂SO₄ (Wako Pure Chemical Industries, Ltd.),
1 M BBr₃ dichloromethane solution (Tokyo Chemical Industry Co, Ltd.),
Boron trifluoride diethyl etherate (≥46% BF₃ basis) (BF₃•Et₂O) (Sigma-Aldrich Co. LLC.),
8-Methylquinoline (Tokyo Chemical Industry Co, Ltd.),
PhI(OAc)₂ (Tokyo Chemical Industry Co, Ltd.),
Pd(OAc)₂ (Tokyo Chemical Industry Co, Ltd.).

2.2. Commercially Available Solvents:

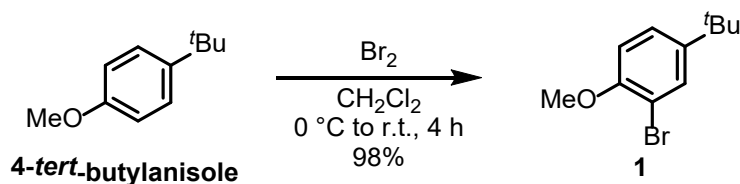
EtOH (Wako Pure Chemical Industries, Ltd.), CHCl₃ (Wako Pure Chemical Industries, Ltd.), hexane (Wako Pure Chemical Industries, Ltd.), EtOAc (Wako Pure Chemical Industries, Ltd.) and CH₂Cl₂ (Wako Pure Chemical Industries, Ltd.) were used without further purification. Deoxidized grade MeOH (Wako Pure Chemical Industries, Ltd.), hexane (Wako Pure Chemical Industries, Ltd.), CH₂Cl₂ (Wako Pure Chemical Industries, Ltd.) and toluene (Wako Pure Chemical Industries, Ltd.) were used without further purification. Triethylamine (Kanto Chemical Co., Inc.) was purified by passage through solvent purification columns under argon pressure.

2.3. Compounds prepared as described in the literature:

8-(Methoxymethyl)quinoline (**4**)¹.

3. Synthetic Procedures and Characterization

3.1. Synthesis of 1



Scheme S1. Synthesis of compound **1**.

4-*tert*-Butylanisole (5.13 g, 31.3 mmol) was dissolved in CH₂Cl₂ (12 ml) and cooled to 0 °C. Bromine (5.00 g, 31.3 mmol) in CH₂Cl₂ (12 ml) was added slowly to the reaction mixture using a dropping funnel under a N₂ atmosphere. After the addition was complete, the mixture was stirred at room temperature for 4 h. Then, the pale yellow solution was quenched by a saturated NaHSO₃ aqueous solution. The product was extracted with CH₂Cl₂. The organic layers were washed with brine, dried over Na₂SO₄, and evaporated to afford **1** as a colorless transparent liquid (7.45 g, 30.1 mmol, 98%).

¹H NMR (CDCl₃, 400 MHz), δ (ppm): 7.54 (d, *J* = 2.3 Hz, 1H), 7.27 (dd, *J* = 8.6, 2.4 Hz, 1H), 6.83 (d, *J* = 8.6 Hz, 1H), 3.88 (s, 3H), 1.29 (s, 9H). The analytical spectral data of ¹H NMR were identical with the literature references.²

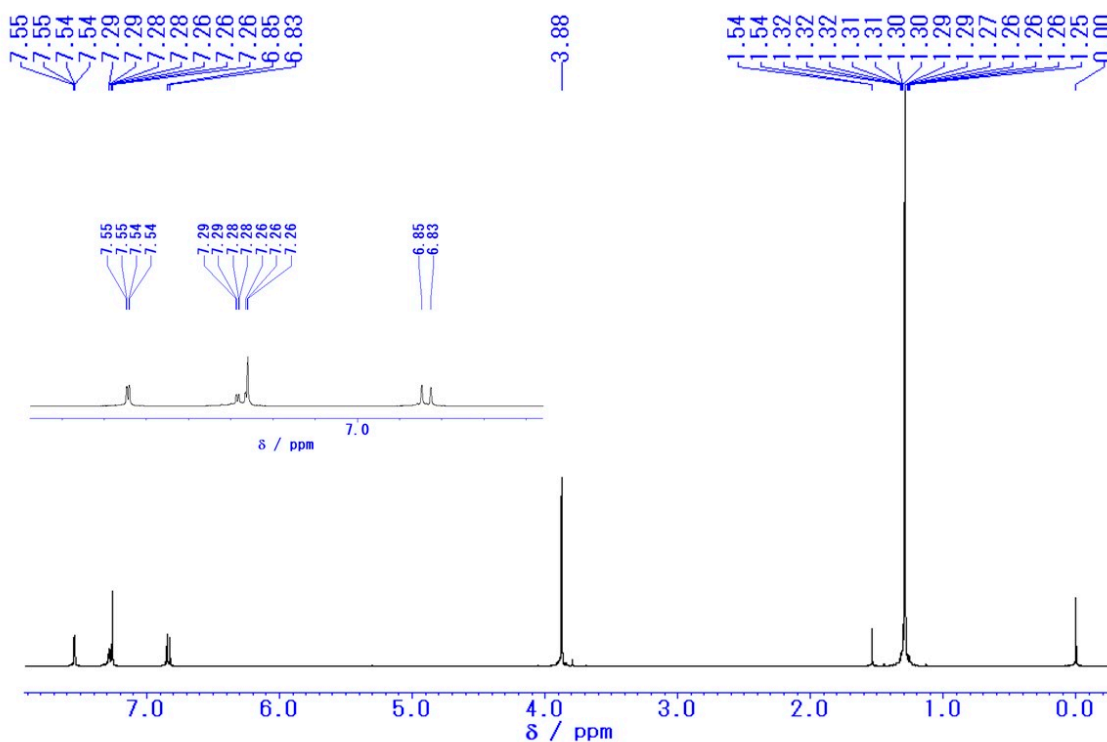
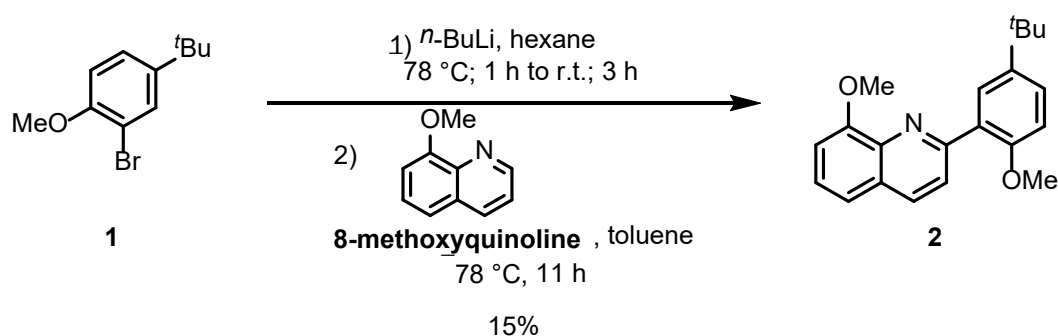


Figure S1. ¹H NMR spectrum of **1**, CDCl₃, 400 MHz.

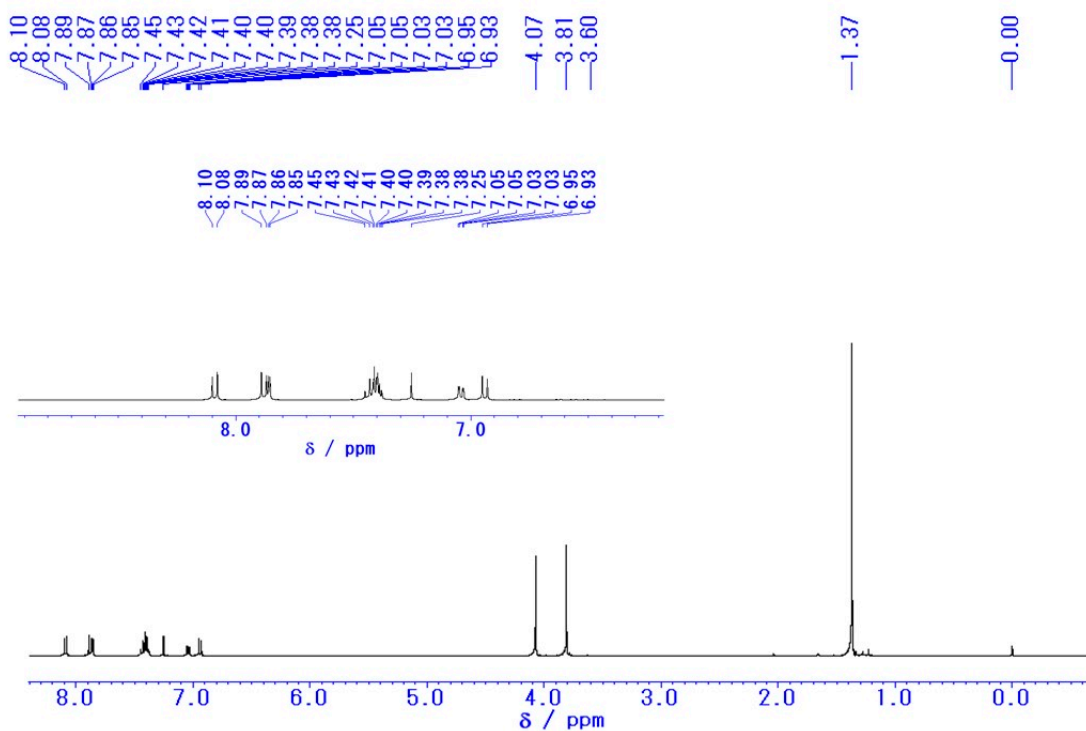
3.2. Synthesis of 2



Scheme S2. Synthesis of compound 2.

1 (1.1 g, 4.53 mmol) was dissolved in hexane (15 mL) and cooled to -78 °C. 1.6 M *n*-BuLi hexane solution (2.8 mL, 4.53 mmol) was added slowly to the reaction mixture under a N_2 atmosphere. The reaction mixture was stirred at -78 °C for 1 h. It formed a yellow suspension, which was stirred at room temperature for 3 h. A solution of 8-methoxyquinoline (0.65 g, 4.11 mmol) in 6 mL of toluene was slowly added to the solution using a dropping funnel. After the addition was complete, the mixture was stirred at room temperature for 10 h. Then, the reaction mixture was quenched by H_2O at 0 °C. The product was extracted with CH_2Cl_2 . The organic layers were washed with brine, dried over Mg_2SO_4 , and the solvent was removed on a rotary evaporator. The residue was purified by column chromatography on SiO_2 (hexane/EtOAc = 4/1 v/v as an eluent) to afford compound 2 as a yellow oil (0.13 g, 0.41 mmol, 9%).

R_f = 0.39 (hexane/EtOAc = 4/1 v/v). HRMS (ESI): calcd. for $[M+H]^+$, 322.1802; found, m/z 322.1807. 1H NMR ($CDCl_3$, 400 MHz), δ (ppm): 8.09 (d, J = 8.5 Hz, 1H), 7.88 (d, J = 8.6 Hz, 1H), 7.86 (d, J = 2.6 Hz, 1H), 7.45–7.37 (m, 3H), 7.04 (dd, J = 7.3, 1.6 Hz, 1H), 6.94 (d, J = 8.6 Hz, 1H), 4.07 (s, 3H), 3.81 (s, 3H), 1.37 (s, 9H). ^{13}C NMR ($CDCl_3$, 100 MHz), δ (ppm): 156.4, 155.6, 155.2, 143.8, 140.2, 134.8, 129.6, 128.7, 128.1, 127.0, 126.2, 124.2, 119.2, 111.3, 107.7, 55.9, 55.9, 34.2, 31.5. The elemental analysis calcd. for $C_{21}H_{23}NO_2$: C, 78.47; H, 7.21; N, 4.36. Found: C, 77.96; H, 7.25; N, 4.39.

Figure S2. 1H NMR spectrum of 2, $CDCl_3$, 400 MHz.

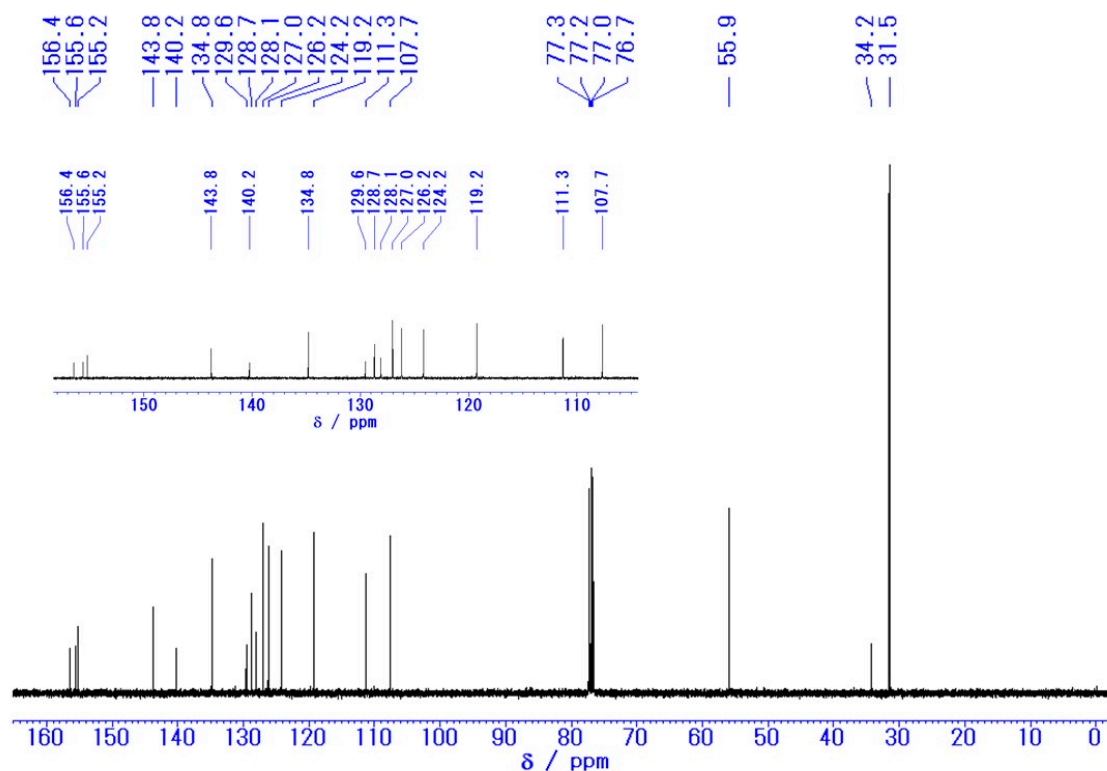
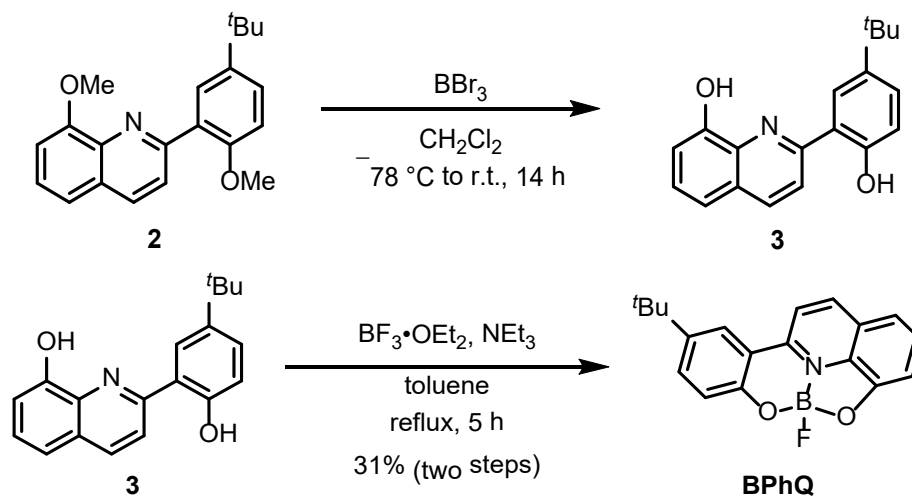


Figure S3. ^{13}C NMR spectrum of **2**, CDCl_3 , 100 MHz.

3.3. Synthesis of BPhQ



Scheme S3. Synthesis of BPhQ.

2 (0.24 g, 0.75 mmol) was dissolved in dry CH_2Cl_2 (5 mL) under a N_2 atmosphere at room temperature, and 1.0 M of BBr_3 (7.5 mL, 7.5 mmol) CH_2Cl_2 solution was then added to the reaction mixture at -78°C . After stirring for 20 h at room temperature, the reaction mixture was quenched by EtOH at 0°C . The solvent was removed on a rotary evaporator to afford crude compound **3** (0.24 g) as a yellow powder. The crude product was used in the next step without any further purification.

3 (0.10 g, 3.41 mmol) was dissolved in 14 mL of dry toluene under a N_2 atmosphere at room temperature, and triethylamine (1.0 mL, 6.83 mmol) was then added to the reaction mixture. $\text{BF}_3\cdot\text{OEt}_2$ (0.9 mL, 6.83 mmol) was added and stirred at 100°C for 19 h. After cooling to room temperature, the reaction mixture was quenched by EtOH and concentrated by a rotary evaporator to give a yellow

powder. The yellow residue was purified by column chromatography on SiO₂ (CH₂Cl₂ as an eluent) to afford **BPhQ** as a yellow solid (0.031 g, 0.10 mmol, 31% from **2**).

R_f = 0.77 (CH₂Cl₂). HRMS (ESI): calcd. for [M+Na]⁺, 302.1247; found, m/z 302.1340. ¹H NMR (CDCl₃, 400 MHz), δ (ppm): 8.53 (d, J = 8.8 Hz, 1H), 7.98 (d, J = 8.8 Hz, 1H), 7.92 (d, J = 2.4 Hz, 1H), 7.66 (dd, J = 8.8, 2.4 Hz, 1H), 7.60 (t, J = 8.3 Hz, 1H), 7.39 (d, J = 8.3 Hz, 1H), 7.33 (d, J = 8.8 Hz, 1H), 7.21 (d, J = 7.6 Hz, 1H), 1.40 (s, 9H). ¹¹B NMR (CDCl₃, 128 MHz), δ (ppm): 5.65 (d, J = 37 MHz). ¹³C NMR (CDCl₃, 100 MHz), δ (ppm): 154.8, 154.1, 146.6, 143.9, 140.6, 134.3, 133.3, 131.1, 125.3, 121.4, 121.4, 117.9, 116.7, 114.5, 111.2, 34.3, 31.3. The elemental analysis calcd. for C₁₉H₁₇BFNO₂: C, 71.06; H, 5.34; N, 4.36. Found: C, 70.90; H, 5.37; N, 4.15.

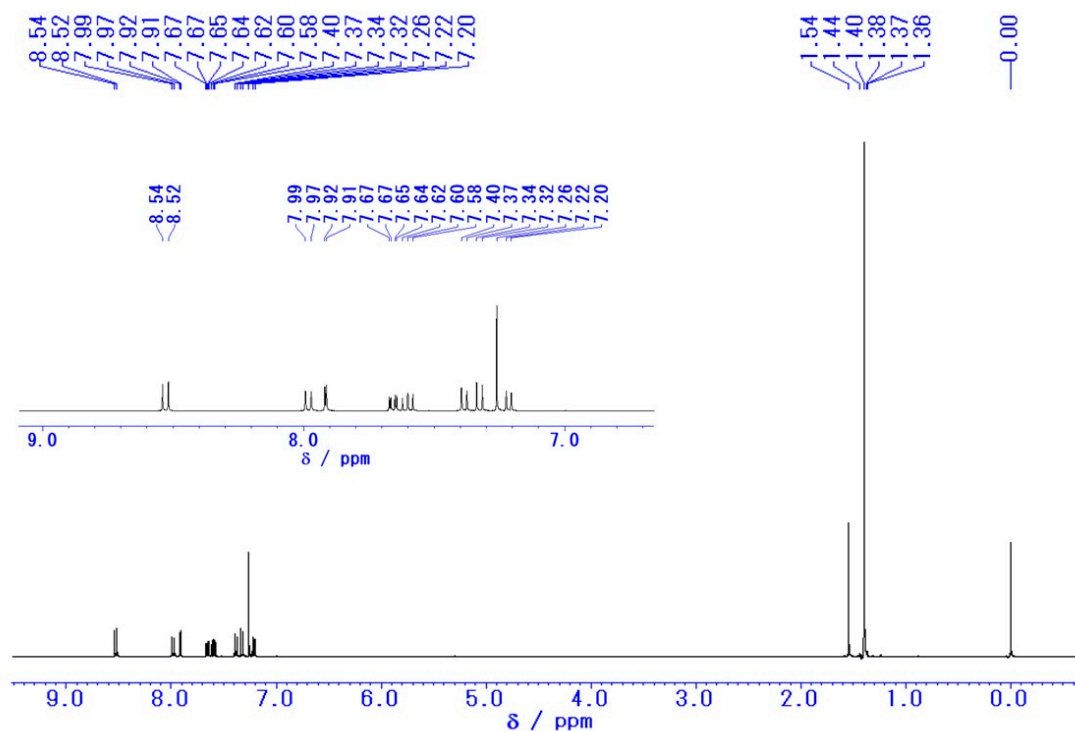


Figure S4. ¹H NMR spectrum of **BPhQ**, CDCl₃, 400 MHz.

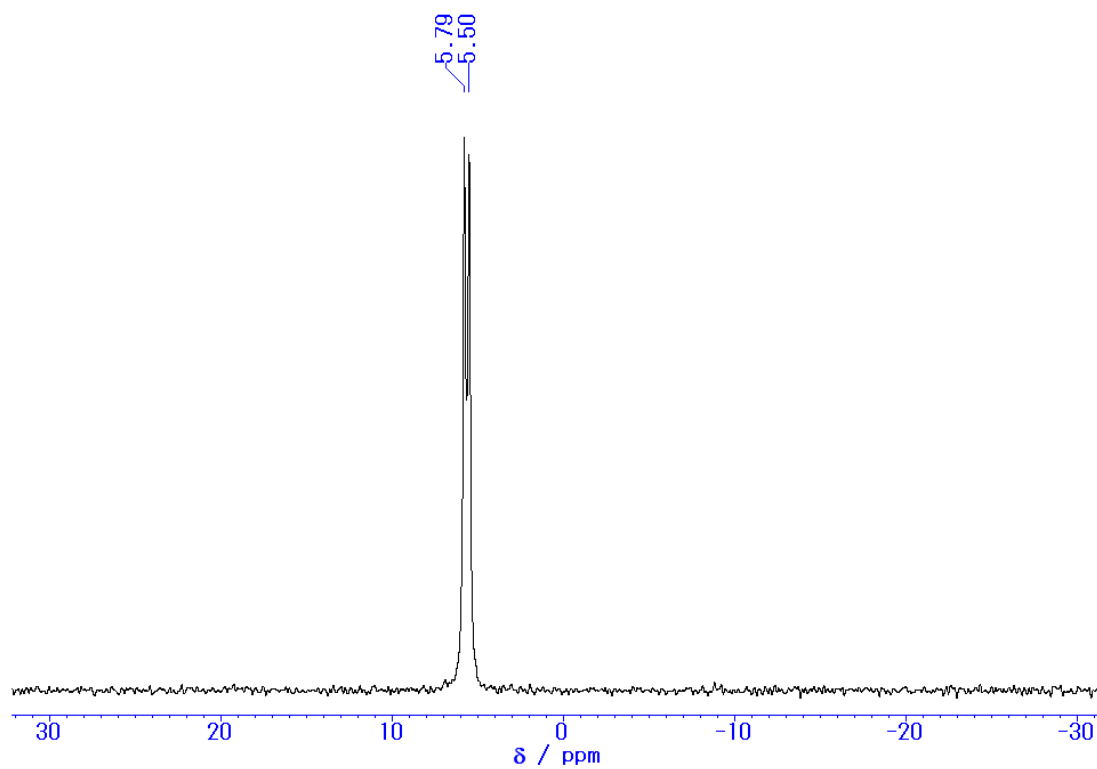


Figure S5. ^{11}B NMR spectrum of BPhQ, CDCl_3 , 128 MHz.

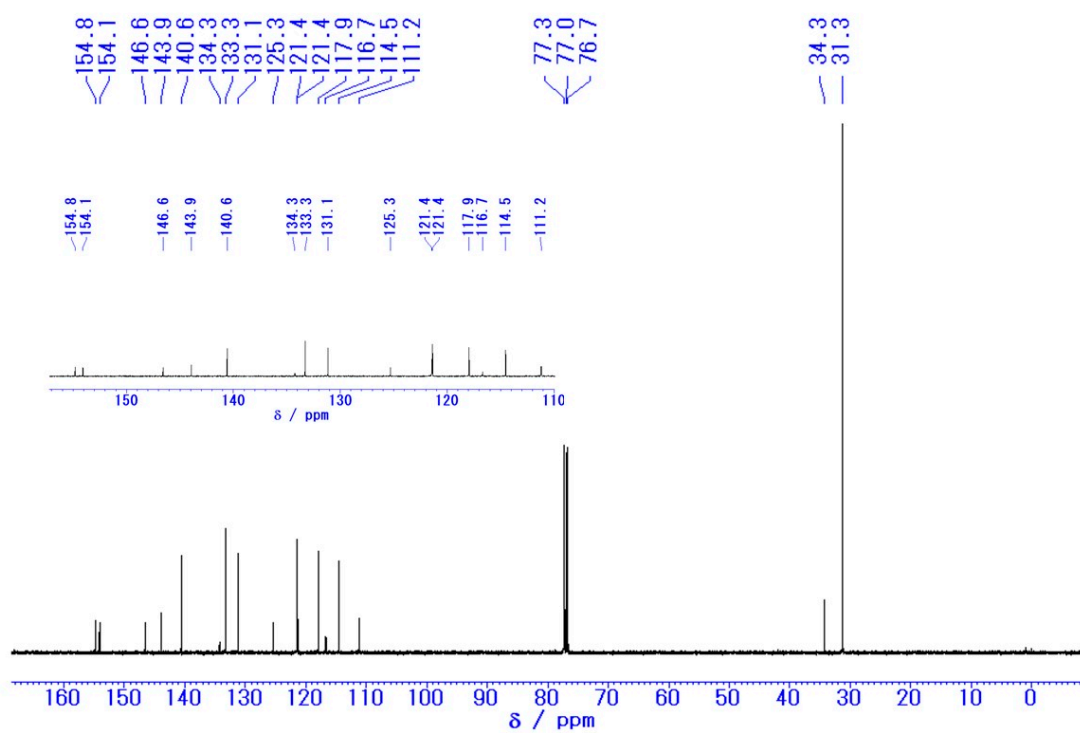
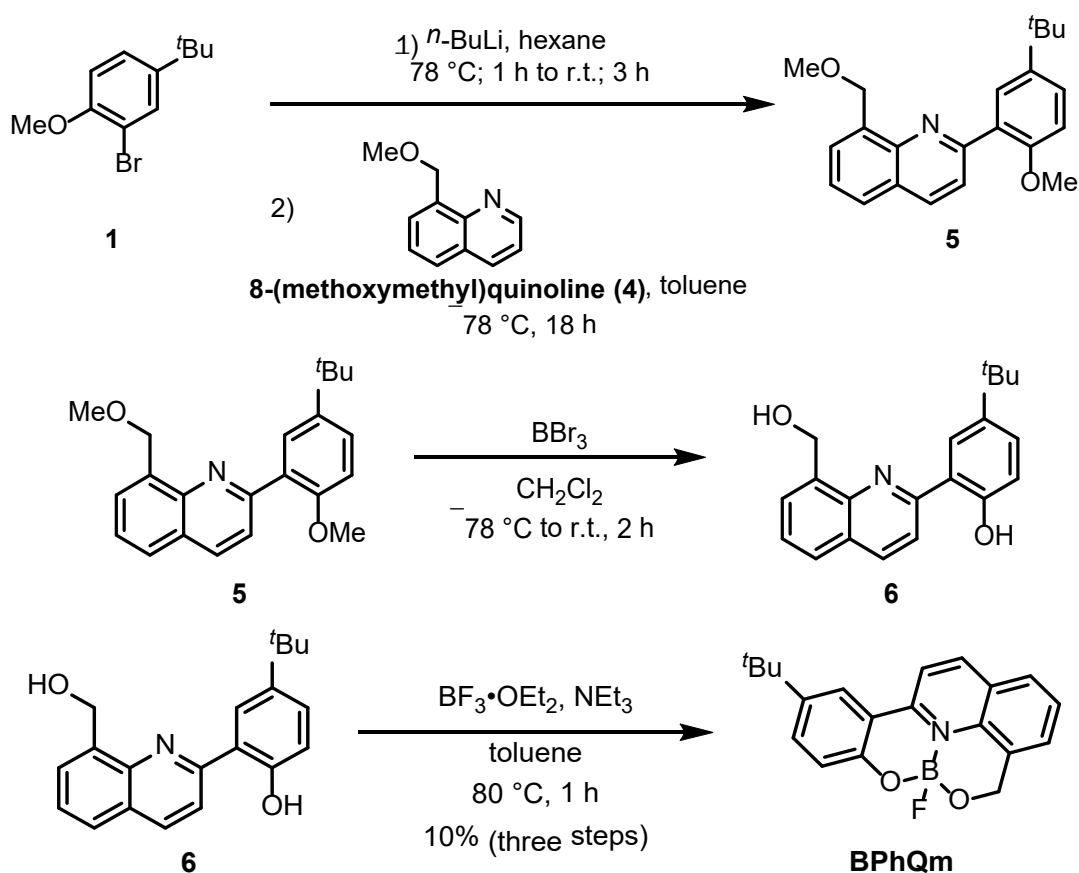


Figure S6. ^{13}C NMR spectrum of BPhQ, CDCl_3 , 100 MHz.

3.4. Synthesis of BPhQm



Scheme S4. Synthesis of BPhQm.

1 (2.7 g, 11.1 mmol) was dissolved in hexane (36 mL) and cooled to -78 °C. 1.6 M of *n*-BuLi hexane solution (6.9 mL, 11.1 mmol) was added slowly to the reaction mixture under a N₂ atmosphere. The reaction mixture was stirred at -78 °C for 1 h. It formed a yellow suspension, which was stirred at room temperature for 3 h. A solution of 8-(methoxymethyl)quinoline (4) (1.75 g, 10.1 mmol) in 15 mL of toluene was slowly added to the solution using a dropping funnel. After the addition was complete, the mixture was stirred at room temperature for 18 h. Then, the reaction mixture was quenched by H₂O at 0 °C. The product was extracted with CH₂Cl₂. The organic layers were washed with brine, dried over Mg₂SO₄, and the solvent was removed on a rotary evaporator. The residue was purified by column chromatography on SiO₂ (hexane/EtOAc = 3/1 v/v as an eluent) to afford crude compound 5 (1.40 g) as a yellow oil. The crude product was used in the next step without any further purification.

5 (1.21 g, 3.61 mmol) was dissolved in dry CH₂Cl₂ (40 mL) under a N₂ atmosphere at room temperature, and 1.0 M of BBr₃ (1.6 mL, 18 mmol) CH₂Cl₂ solution was then added to the reaction mixture at -78 °C. After stirring for 2 h at room temperature, the reaction mixture was quenched by H₂O at 0 °C. The product was extracted with CH₂Cl₂. The organic layers were washed with brine, dried over Mg₂SO₄, and the solvent was removed on a rotary evaporator to afford crude compound 6 (1.29 g) as a yellow solid. The crude product was used in the next step without any further purification.

6 (1.29 g, 4.20 mmol) was dissolved in 125 mL of dry toluene under a N₂ atmosphere at room temperature, and triethylamine (1.2 mL, 8.39 mmol) was then added to the reaction mixture. BF₃·OEt₂ (1.6 mL, 12.6 mmol) was added and stirred at 80 °C for 1 h. After cooling to room temperature, the reaction mixture was quenched by EtOH and concentrated by a rotary evaporator to give a yellow powder. The residue was purified by column chromatography on SiO₂ (hexane/EtOAc = 1/1 v/v as an eluent) to afford a yellow solid (1.40 g). The yellow residue was purified by reprecipitation with

CHCl_3 and hexane (good and poor solvent, respectively) to afford **BPhQm** (0.14 g, 10%, three steps from **1**) as a yellow powder.

$R_f = 0.24$ (hexane/EtOAc = 1/1 v/v). HRMS (ESI): Calcd for $[\text{M}+\text{Na}]^+$, 358.1385; found, m/z 358.1385. ^1H NMR (CDCl_3 , 400 MHz), δ (ppm): 8.50 (d, $J = 9.0$ Hz, 1H), 8.13 (d, $J = 9.0$ Hz, 1H), 7.91 (d, $J = 2.3$ Hz, 1H), 7.84–7.82 (m, 1H), 7.67–7.60 (m, 3H), 7.20 (d, $J = 8.7$ Hz, 1H), 5.67 (d, $J = 15$ Hz, 1H), 5.23 (d, $J = 15$ Hz, 1H), 1.39 (s, 9H). ^{11}B NMR (CDCl_3 , 128 MHz), δ (ppm): 1.69 (d, $J = 41$ MHz). ^{13}C NMR (CDCl_3 , 100 MHz), δ (ppm): 155.7, 149.5, 143.0, 141.4, 136.7, 133.2, 132.7, 128.2, 127.4, 126.9, 126.4, 122.3, 120.5, 117.2, 116.4, 62.6 (d, $J = 4.1$ Hz), 34.4, 31.4. The elemental analysis calcd. for $\text{C}_{20}\text{H}_{19}\text{BFNO}_2$: C, 71.67; H, 5.71; N, 4.18. Found: C, 71.50; H, 5.90; N, 4.11.

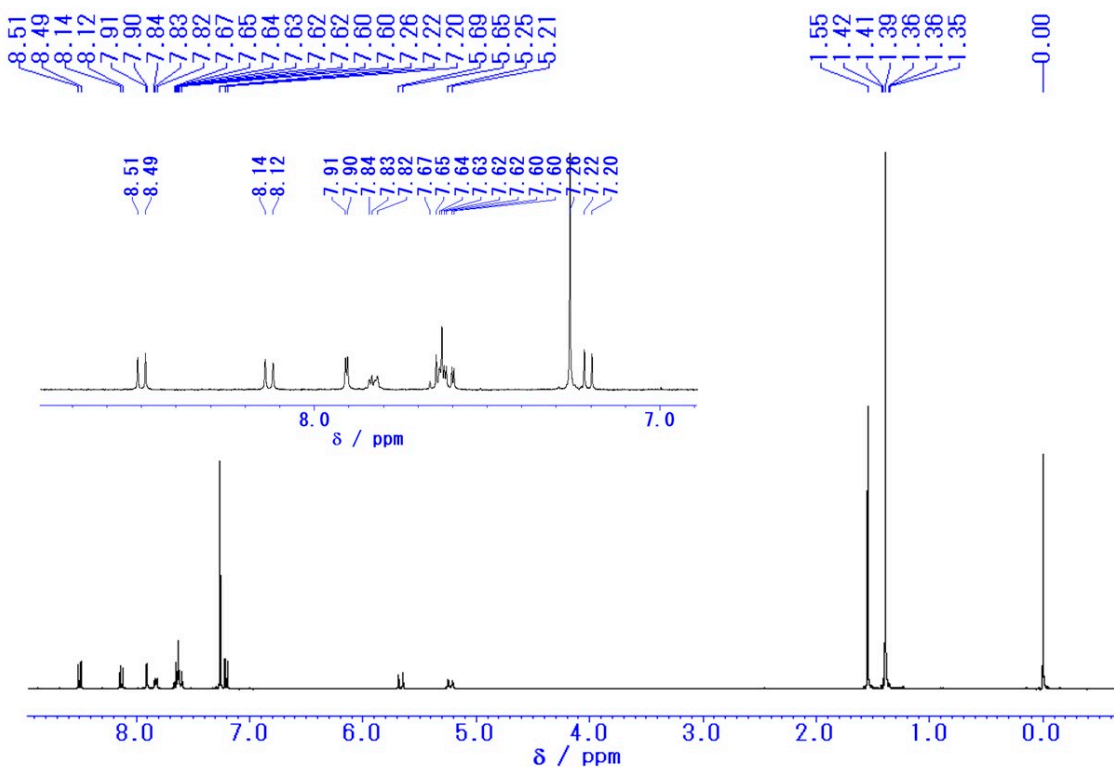
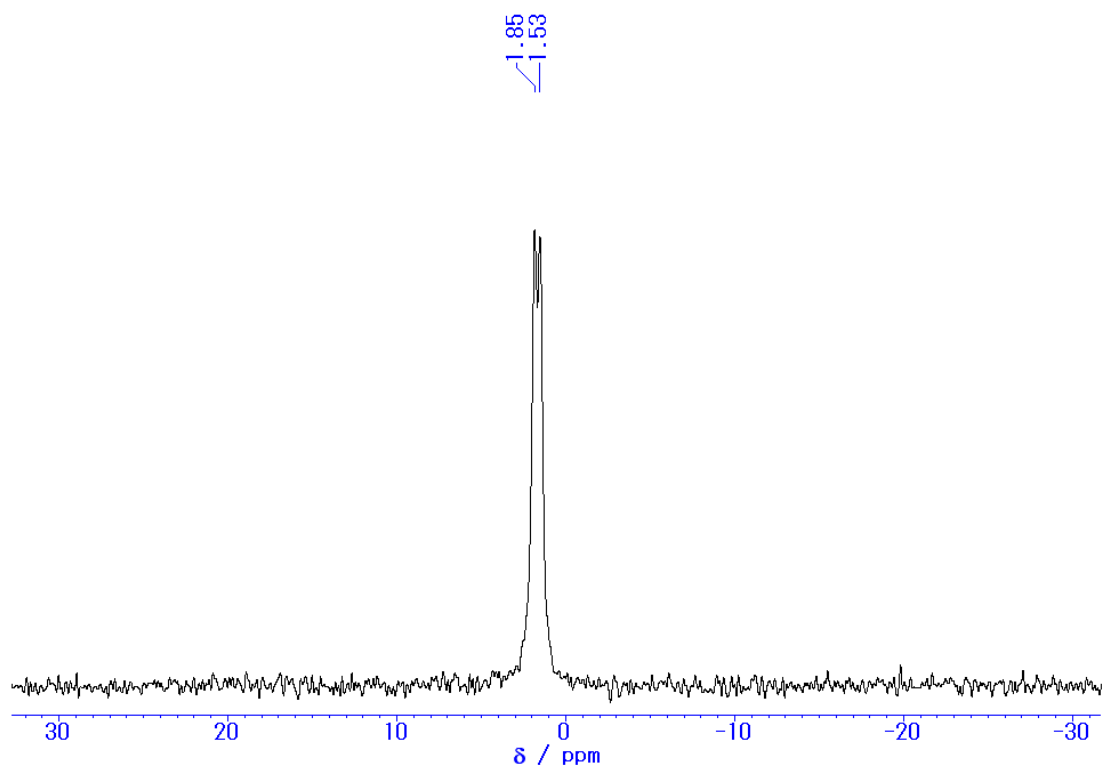
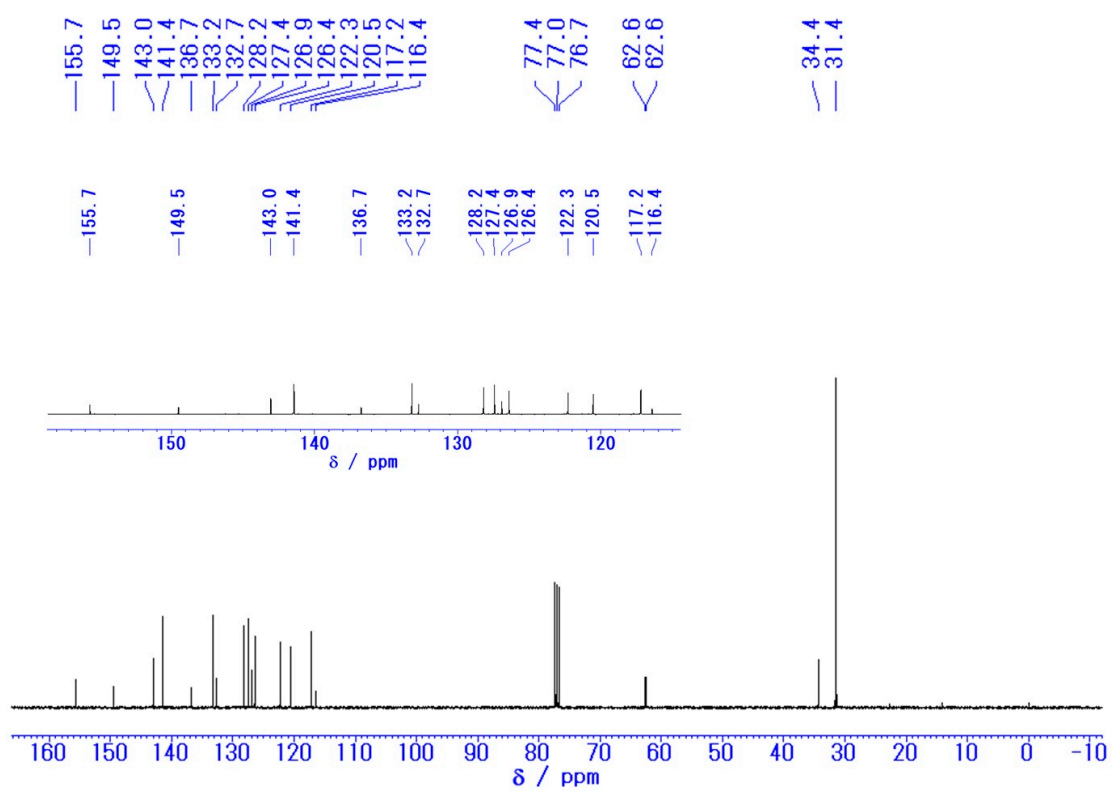


Figure S7. ^1H NMR spectrum of **BPhQm**, CDCl_3 , 400 MHz.

Figure S8. ^{11}B NMR spectrum of **BPhQm**, CDCl_3 , 128 MHz.Figure S9. ^{13}C NMR spectrum of **BPhQm**, CDCl_3 , 100 MHz.

4. X-ray Crystal Structure Analysis of BPhQ

Intensity data were collected on a Rigaku R-Axis RAPID imaging plate area detector with graphite monochromated MoK α radiation ($\lambda = 0.71069 \text{ \AA}$). The structures were solved and refined by full-matrix least-squares procedures based on F^2 (SHELXL-2014/7).

A single crystal of **BPhQ** was prepared by the vapor diffusion method from the CH₂Cl₂ solution under a hexane atmosphere at room temperature.

Table S1. Crystallographic data of BPhQ at 93 K	
Morphology	yellow block
Space group	<i>P</i> 1
<i>a</i> / \AA	7.4997 (13)
<i>b</i> / \AA	10.0459 (17)
<i>c</i> / \AA	11.063 (2)
α /deg	70.034 (5)
β /deg	87.722 (6)
γ /deg	86.054 (6)
<i>V</i> / \AA^3	781.4 (2)
<i>Z</i>	2
Density/g cm ⁻³	1.365
Absorption coefficient	0.095
<i>F</i> (000)	892
Crystal size (nm)	0.500 × 0.300 × 0.300
θ range for data collection	3.327–27.475
Limiting indices	-9 ≤ <i>h</i> ≤ 9, -13 ≤ <i>k</i> ≤ 11, -14 ≤ <i>l</i> ≤ 14
Reflections collected (unique)	3567/2912 [R(int) = 0.060]
Completeness to $\theta = 27.475$	0.994
Max. and min. transmission	1.000 and 0.229
Goodness-off-fit on F^2	1.063
Final R indices [<i>I</i> > 2 σ (<i>I</i>)] ^a	<i>R</i> ₁ = 0.0563 <i>wR</i> ₂ = 0.1565
R indices (all data)	<i>R</i> ₁ = 0.0665 <i>wR</i> ₂ = 0.1466
<i>T</i> /K	93

[a] $R_1 = \frac{\sum(|F_o| - |F_c|)}{\sum|F_o|}$. $wR_2 = \left[\frac{\sum w(F_o^2 - F_c^2)^2}{\sum w(F_o^2)^2} \right]^{1/2}$. $w = 1/[\sigma^2(F_o^2) + (ap)^2 + bp]$, where $p = [\max(F_o^2, 0) + 2F_c^2]/3$.

5. X-ray Crystal Structure Analysis of BPhQm

The intensity data were collected on a Rigaku Saturn 724+ with MicroMax-007HF CCD diffractometer with Varimax Mo optics using graphite-monochromated MoK α radiation. The structures were solved and refined by full-matrix least-squares procedures based on F^2 (SHELXL-2014/7).

A single crystal of **BPhQm** was prepared by the vapor diffusion method. **BPhQm** was dissolved into toluene by heating. The single crystal was obtained from the solution under a hexane atmosphere at room temperature.

Table S2. Crystallographic data of **BPhQm** at 143 K

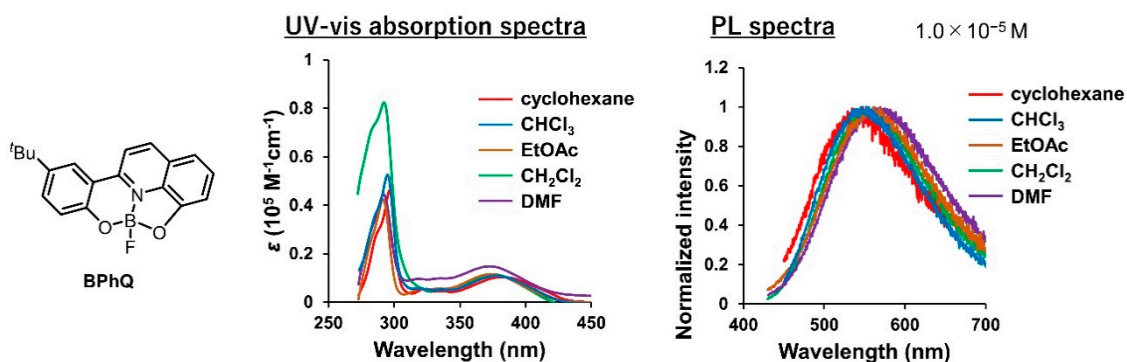
Morphology	yellow plate
Space group	<i>P</i> 1
<i>a</i> /Å	7.211(8)
<i>b</i> /Å	8.520(8)
<i>c</i> /Å	13.549(14)
α /deg	99.116(17)
β /deg	103.179(15)
γ /deg	96.001(12)
<i>V</i> /Å ³	791.6(14)
<i>Z</i>	2
Density/g cm ⁻³	1.406
Absorption coefficient	0.097
<i>F</i> (000)	352
Crystal size (nm)	0.150 × 0.060 × 0.020
θ range for data collection	3.145–27.486
Limiting indices	-8 ≤ <i>h</i> ≤ 9, -11 ≤ <i>k</i> ≤ 10, -17 ≤ <i>l</i> ≤ 17
Reflections collected (unique)	349/1991 [R(int) = 0.057]
Completeness to $\theta = 27.486$	0.951
Max. and min. transmission	1.000 and 0.321
Goodness-off-fit on F^2	0.912
Final R indices [<i>I</i> > 2 σ (<i>I</i>)] ^a	<i>R</i> ₁ = 0.0631 <i>wR</i> ₂ = 0.1508
R indices (all data)	<i>R</i> ₁ = 0.1145 <i>wR</i> ₂ = 0.1883
<i>T</i> /K	143

$$[a] R_1 = \frac{\sum(|F_o| - |F_c|)}{\sum|F_o|}, \quad wR_2 = \left[\frac{\sum w(F_o^2 - F_c^2)^2}{\sum w(F_o^2)^2} \right]^{1/2}, \quad w = 1/[\sigma^2(F_o^2) + (ap)^2 + bp], \quad \text{where } p = [\max(F_o^2, 0) + 2F_c^2]/3.$$

6. Optical Measurement Data

6.1. Solvatochromism Study

6.1.1. BPhQ



	Δf^a	$\lambda_{\text{max,abs}} \text{ (nm)}^b$	$\lambda_{\text{em}} \text{ (nm)}^c$	Φ_F^d
cyclohexane ^e	-0.0014	383	542	0.002
CHCl ₃	0.15	377	550	0.008
EtOAc ^e	0.20	374	561	0.006
CH ₂ Cl ₂ ^e	0.22	375	556	0.007
DMF ^e	0.27	372	567	0.007

^aOrientation polarizability.

^bThe longest absorption maximum.

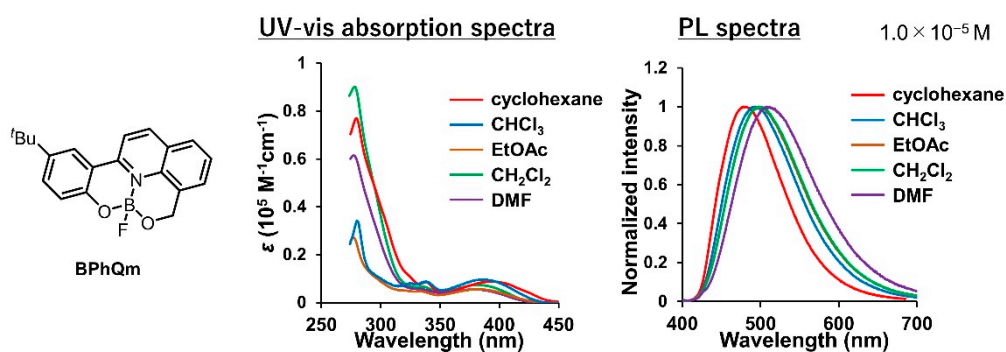
^cFluorescence maxima with the excitation at the longest absorption maximum.

^dAbsolute fluorescence quantum efficiencies.

^eCHCl₃/solvent = 1/99 v/v (1.0 × 10⁻⁵ M).

Figure S10. UV-vis absorption (left) and PL spectra (right) of **BPhQ** in the diluted solutions (1.0 × 10⁻⁵ M) at room temperature.

6.1.2. BPhQm



	Δf^a	$\lambda_{\text{max,abs}} \text{ (nm)}^b$	$\lambda_{\text{cm}} \text{ (nm)}^c$	Φ_F^d
cyclohexane ^e	-0.0014	395	478	0.14
CHCl ₃	0.15	387	493	0.21
EtOAc ^e	0.20	383	497	0.17
CH ₂ Cl ₂ ^e	0.22	382	500	0.19
DMF ^e	0.27	379	512	0.17

^aOrientation polarizability.

^bThe longest absorption maximum.

^cFluorescence maxima with the excitation at the longest absorption maximum.

^dAbsolute fluorescence quantum efficiencies.

^eCHCl₃/solvent = 1/99 v/v (1.0 × 10⁻⁵ M).

Figure S11. UV-vis absorption (left) and PL spectra (right) of BPhQm in the diluted solutions (1.0×10⁻⁵ M) at room temperature.

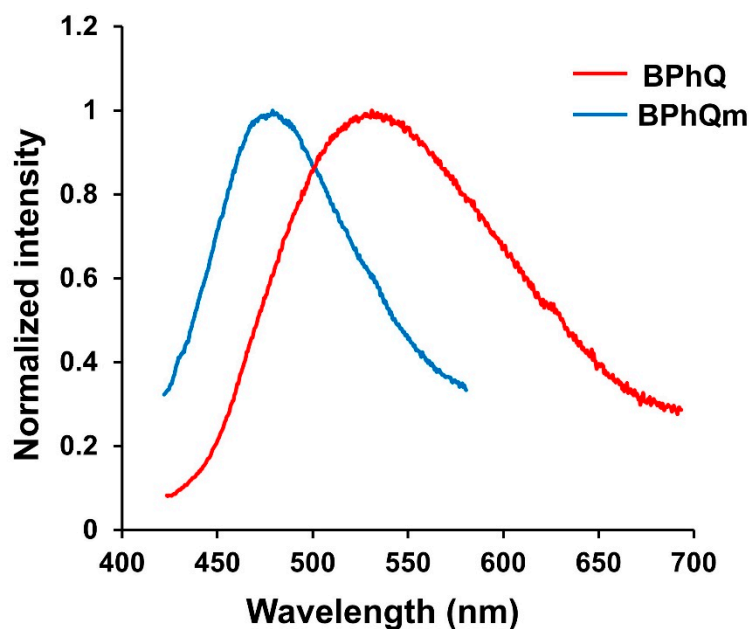


Figure S12. PL spectra of BPhQ and BPhQm in the 1 wt% polystyrene dispersed films.

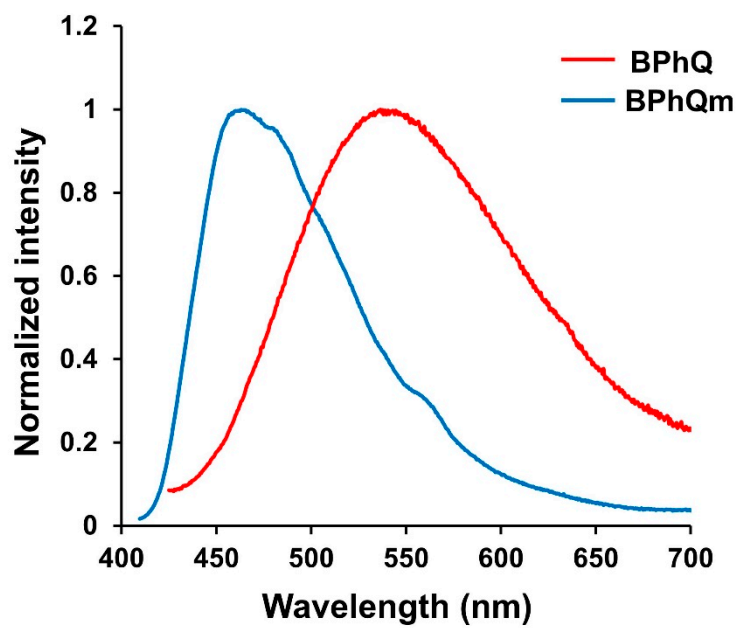


Figure S13. PL spectra of BPhQ and BPhQm in aggregated states (THF/H₂O = 1/99, 1.0×10⁻⁴ M).

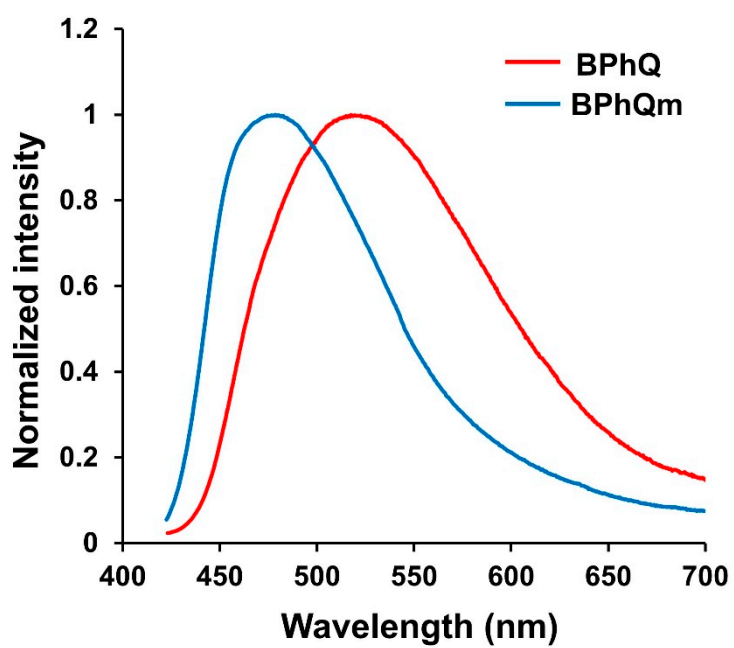


Figure S14. PL spectra of BPhQ and BPhQm in crystalline states.

6.2 PL Lifetime Decay Curves

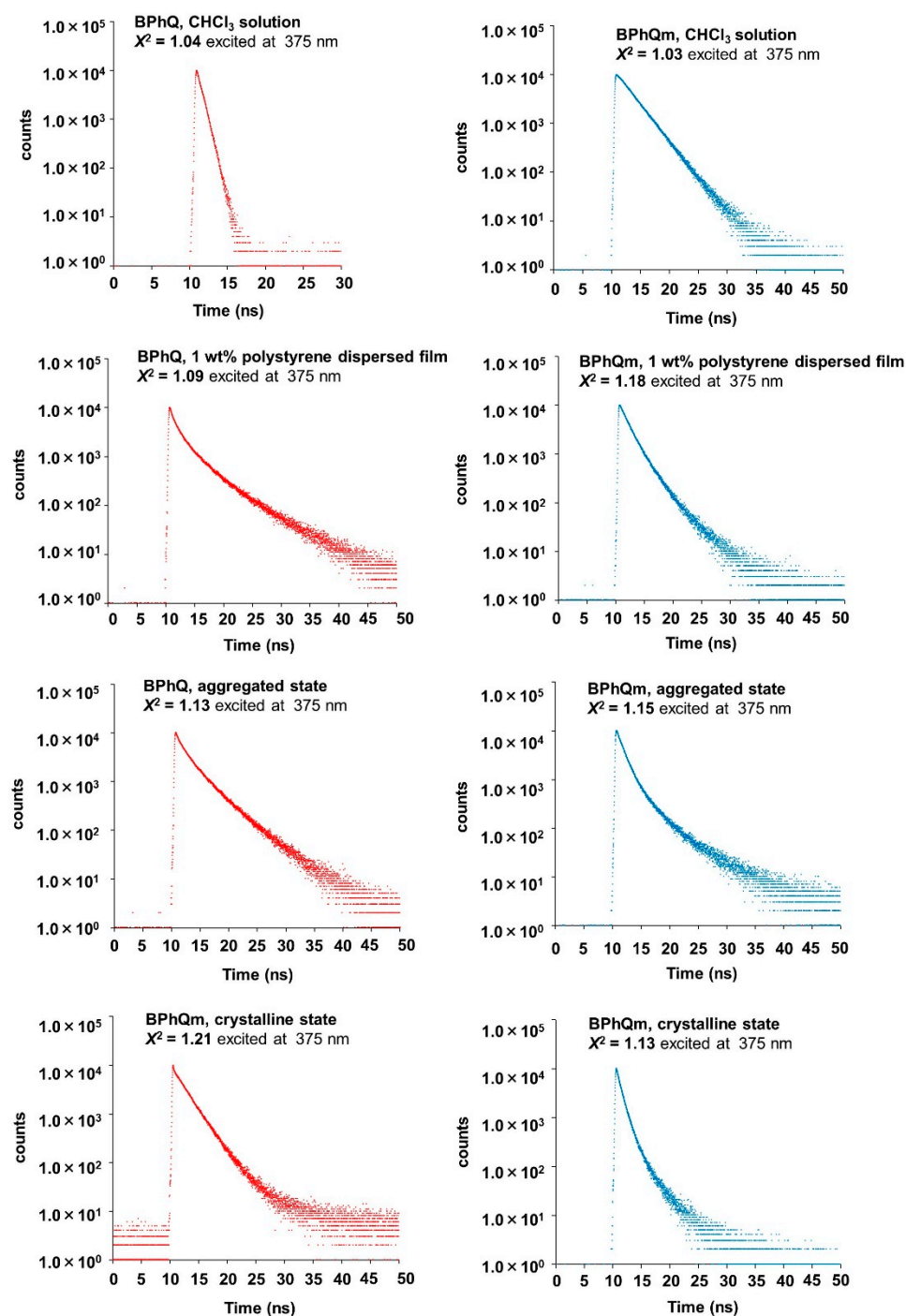


Figure S15. PL lifetime decay curves of BPhQ and BPhQm in chloroform solution (1.0×10^{-5} M), 1 wt% polystyrene film, the aggregated and crystalline states at room temperature. Their emissions at the PL peak tops were monitored.

7. Computational Details

The Gaussian 09 program package³ was used for computation. We optimized the structures of **BPhQ** and **BPhQm** in the excited S_1 states and calculated their molecular orbitals. DFT was applied for the optimization of the structures in the S_0 states at the B3LYP/6-311G(d,p) level and for the S_1 states at the B3LYP/6-311 + G(d,p) level.

References

1. Dick, A. R.; Hull, K. L.; Sanford, M. S. *J. Am. Chem. Soc.* **2004**, *126*, 2300–2301.
2. Zhang, Z.; Chen, Y.-A.; Hung, W.-Y.; Tang, W.-F.; Hsu, Y.-H.; Chen, C.-L.; Meng, F.-Y.; Chou, P.-T. *Chem. Mater.* **2016**, *28*, 8815–8824.
3. Gaussian 09, Revision D.01, Frisch, M. J.; Trucks, G. W.; Schlegel, H. B.; Scuseria, G. E.; Robb, M. A.; Cheeseman, J. R.; Scalmani, G.; Barone, V.; Mennucci, B.; Petersson, G. A.; Nakatsuji, H.; Caricato, M.; Li, X.; Hratchian, H. P.; Izmaylov, A. F.; Bloino, J.; Zheng, G.; Sonnenberg, J. L.; Hada, M.; Ehara, M.; Toyota, K.; Fukuda, R.; Hasegawa, J.; Ishida, M.; Nakajima, T.; Honda, Y.; Kitao, O.; Nakai, H.; Vreven, T.; Montgomery, Jr., J. A.; Peralta, J. E.; Ogliaro, F.; Bearpark, M.; Heyd, J. J.; Brothers, E.; Kudin, K. N.; Staroverov, V. N.; Kobayashi, R.; Normand, J.; Raghavachari, K.; Rendell, A.; Burant, J. C. S.; Iyengar, S.; Tomasi, J.; Cossi, M.; Rega, N.; Millam, J. M.; Klene, M.; Knox, J. E.; Cross, J. B.; Bakken, V.; Adamo, C.; Jaramillo, J.; Gomperts, R.; Stratmann, R. E.; Yazyev, O.; Austin, A. J.; Cammi, R.; Pomelli, C.; Ochterski, J. W.; Martin, R. L.; Morokuma, K.; Zakrzewski, V. G.; Voth, G. A.; Salvador, P.; Dapprich, S.; Daniels, A. D.; Farkas, Ö.; Foresman, J. B.; Ortiz, J. V.; Cioslowski, J.; Fox, D. J. Gaussian, Inc., Wallingford CT, 2009.



© 2020 by the authors. Submitted for possible open access publication under the terms and conditions of the Creative Commons Attribution (CC BY) license (<http://creativecommons.org/licenses/by/4.0/>).